Map-Subtraction Based Moving-Object Tracking with Motorcycle-Mounted Scanning LiDAR

Ibuki YOSHIDA*, Shotaro MURO**, Masafumi HASHIMOTO***, and Kazuhiko TAKAHASHI***

(Received September 28, 2021)

This paper presents a method for tracking (estimation of position, velocity and size) of moving objects, such as cars, motorcycles, and pedestrians, in global navigation satellite systems (GNSS)-denied environments using light detection and ranging (LiDAR) mounted on motorcycle. 3D-point cloud environmental map is assumed to be acquired in advance. Distortion in scan data from the scanning LiDAR is corrected by estimating the pose (3D positions and attitude angles) of the motorcycle in a period shorter than the LiDAR scan period using normal distribution transforms (NDT) based map matching and the information from inertial measurement unit (IMU) via the extended Kalman filter (EKF). The corrected LiDAR scan data are compared with environmental map, and the LiDAR scan data of interest are extracted from the current LiDAR scan data based on map-subtraction method. The extracted scan data are mapped onto an elevation map, and moving objects are detected based on an occupancy grid method. Finally, detected moving objects are tracked based on the Bayesian Filter. Experimental results obtained in public road and university-campus road environments validate the effectiveness of the proposed method.

Key words：LiDAR, moving-object tracking, motorcycle, map subtraction

1. Introduction

In mobile robotics and vehicle automation domains, tracking (estimation of position, velocity, and size) of moving objects, such as cars, motorcycles, and pedestrians, is an important technology to achieve the advanced driver assistant system (ADAS) and autonomous driving. A lot of studies of moving-object tracking using cameras, light detection and rangings (LiDARs), and radars have been actively conducted [1-3].

When compared with camera-based tracking, LiDAR-based tracking is robust to lighting conditions and require less computational time. Furthermore, LiDAR-based tracking provides tracking accuracy better than radar-based tracking due to higher spatial resolution of LiDAR. From these reasons, we have presented a LiDAR-based tracking of moving objects [4, 5].

Most methods of moving-object tracking have been applied to ADAS and autonomous driving for cars and trucks (four-wheeled vehicles) traveling on flat road surfaces. Although moving-object tracking is required for advanced rider assist systems (ARAS) for motorcycles, there are few studies on moving-object tracking with motorcycle-mounted sensors [6-9].

This paper presents a method of moving-object tracking using a scanning LiDAR mounted on a motorcycle. Moving-object tracking by a motorcycle-mounted LiDAR is more difficult than that by a four-wheeled vehicle-mounted LiDAR. Because the attitude of a motorcycle changes more drastically than that of a four-wheeled vehicle, the sensing accuracy deteriorates.

The occupancy grid method [10], in which the grid map is represented in the world coordinate frame, is usually applied to moving-object detection and tracking.

*Graduate School of Science and Engineering, Doshisha University, Kyoto E-mail: ctwg0157@mail4.doshisha.ac.jp
**Graduate School of Science and Engineering, Doshisha University, Kyoto. Currently, Komatsu Ltd., Tokyo
***Department of Science and Engineering, Doshisha University, Kyoto E-mail: {mhashimo, katakaha}@mail.doshisha.ac.jp

In order to perform accurate moving-object detection, it is necessary to accurately map LiDAR scan data obtained in the sensor coordinate frame onto a grid map using a vehicle's pose (position and attitude angle). Since the LiDAR obtains data by the laser scanning, all scan data within one scan cannot be obtained at the same time when the vehicle is moving or changing its own attitude. Therefore, if all scan data within one scan are mapped onto the world coordinate frame using the pose of the vehicle at a single time, distortion in the LiDAR scan data occurs [11]. In addition, when the LiDAR is mounted on a motorcycle, the mapping accuracy deteriorates due to the large swing motion of the LiDAR. As a result, undetection and false detection of moving objects increase.

In order to address these problems, our previous work [12] presented a moving-object tracking using a bicycle-mounted scanning LiDAR in open-sky environments. The self-pose of the bicycle was estimated every shorter period than LiDAR scan period using the pose information from global navigation satellite systems (GNSS)/inertial navigation system (INS) unit, and then using the pose estimates, the distortion in LiDAR scan data was corrected.

Furthermore, the differences (subtracted scan data) were extracted between the current LiDAR scan data and the 3D-point cloud environment map, and only the subtracted scan data were mapped onto the grid map to accurately perform moving-object detection and tracking. The 3D-point cloud environment map were acquired in advance by our LiDAR-based simultaneous localization and mapping (SLAM)[13,14]. The effectiveness of the method was validated through experimental results obtained in open-sky environments.

However, further improvement to our tracking system is needed. Although our previous work utilized the self-pose information from GNSS, the accuracy of GNSS positioning was decreased in urban and mountainous areas due to the blockage, reflection, and diffraction caused by buildings and mountains. To work well our moving-object tracking in GNSS-denied environments, in this paper, distortion in LiDAR scan data is corrected using normal distribution transforms (NDT) based map matching and the information from inertial measurement unit (IMU) via the extended Kalman filter (EKF) [15]. In addition, this paper presents a moving-object tracking using motorcycle-mounted scanning LiDAR. Thus, this paper is an extension of our previous work [12] on map-subtraction based moving-object tracking, which used a bicycle-mounted scanning LiDAR in GNSS environments.

The rest of this paper is organized as follows. In Section 2, an overview of the experimental system is given. In Section 3, the method of distortion correction is described. In Section 4, method of detecting and tracking moving objects is described. In Section 5, experimental results are presented, followed by conclusions and future works in Section 6.

2. Experimental System

Fig. 1 shows an overview of our experimental motorcycle (Honda, Gyro Canopy). The top part of the motorcycle is equipped with a 32-layer LiDAR (Velodyne, HDL-32E) and an IMU (Xsens, MTi-300). The maximum range of the LiDAR is 70 m, the horizontal viewing angle is 360° with a resolution of 0.16°, and the vertical viewing angle is 41.34° with a resolution of 1.33°. LiDAR acquires 384 measurements (the 3D position of the object and reflection intensity) every 0.55 ms (at 2° horizontal angle increments). The period for the LiDAR beam to complete one rotation (360°) in the horizontal direction is 100 ms, and 70,000 measurements are then acquired in one rotation.

The IMU outputs the attitude angle (roll and pitch angles) and angular velocity (roll, pitch, and yaw angular velocities) every 10 ms. The error in attitude angle and the angular velocity are less than +-0.3° and +-0.2°/s, respectively.

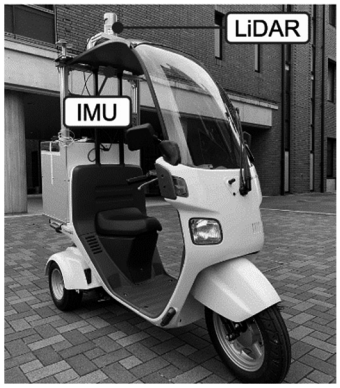

Fig. 1. Experimental system.

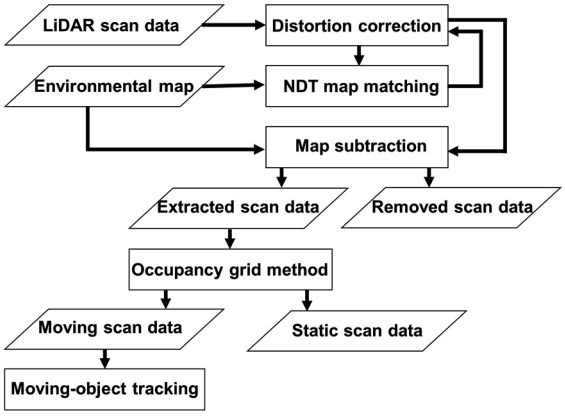

Fig. 2. Flow of moving-object tracking.

3. Distortion Correction of LiDAR scan data

3.1 *NDT map matching*

Fig. 2 shows the flow of moving-object tracking. For moving-object tracking, the LiDAR scan data are mapped from the sensor coordinate frame onto the world coordinate frame using the self-pose (3D position and attitude angle) information of the motorcycle. For this, the accurate self-pose of the motorcycle is required. 3D point-cloud environmental map acquired in advance by our LiDAR-based SLAM [13,14] is implemented on the motorcycle, and NDT map matching [16] is then used to estimate the self-pose in GNSS-denied environments as follows.

For the i-th ($i = 1, 2, \ldots, n$) measurement in the scan data, the position vector in the sensor coordinate frame is defined as $\boldsymbol{p}_{bi} = (x_{bi}, y_{bi}, z_{bi})^T$, and that in the world coordinate frame as $\boldsymbol{p}_i = (x_i, y_i, z_i)^T$. The following relation is then given:

$$\begin{pmatrix} \boldsymbol{p}_i \\ 1 \end{pmatrix} = T(\boldsymbol{X}) \begin{pmatrix} \boldsymbol{p}_{bi} \\ 1 \end{pmatrix} \tag{1}$$

where $\boldsymbol{X} = (x, y, z, \phi, \theta, \psi)^T$ is the pose of the motorcycle. $(x, y, z)^T$ and $(\phi, \theta, \psi)^T$ are the 3D position and attitude angle (roll, pitch, and yaw angles), respectively, of the motorcycle in the world coordinate frame. $T(\boldsymbol{X})$ is the homogenous transformation matrix as follows:

$$T(\mathbf{X}) = \begin{pmatrix} \cos\theta\cos\psi & \sin\phi\sin\theta\cos\psi - \cos\phi\sin\psi & \cos\phi\sin\theta\cos\psi + \sin\phi\sin\psi & x \\ \cos\theta\sin\psi & \sin\phi\sin\theta\sin\psi + \cos\phi\cos\psi & \cos\phi\sin\theta\sin\psi - \sin\phi\cos\psi & y \\ -\sin\theta & \sin\phi\cos\theta & \cos\phi\cos\theta & z \\ 0 & 0 & 0 & 1 \end{pmatrix}$$

NDT map matching matches the current scan data that are obtained at the current time with the environment map using NDT scan matching. NDT scan matching conducts a normal distribution transformation for the LiDAR measurements (3D positions) in each voxel of the environmental map. It calculates the mean and covariance of LiDAR measurements of the environmental map. The pose of the motorcycle, $\boldsymbol{X}$, can be calculated by maximizing the following likelihood function:

$$\Lambda = \prod_{i=1}^{n} \exp\left(-\frac{1}{2} (\boldsymbol{p}_i'(t) - \boldsymbol{q}_i)^T \boldsymbol{\Omega}_i^{-1} (\boldsymbol{p}_i'(t) - \boldsymbol{q}_i) \right) \tag{2}$$

where $\boldsymbol{q}_i$ and $\boldsymbol{\Omega}_i$ are the mean and covariance, respectively, of the LiDAR measurement positions in the i-th voxel of the environmental map. $\boldsymbol{p}_i'(t)$ is the current scan data in the i-th voxel.

Since the environmental map and the current scan data contain a lot of scan data, it takes much computational cost for the NDT map matching. Therefore, to reduce the computational cost, a voxel grid filter [17] is applied to downsize scan data related to the environment map and current scan data. Thereafter, scan data are mapped onto the 3D grid map (voxel map). Here, the voxel used for the voxel grid filter is a cube with a side length of 0.2 m, whereas the voxel for the voxel map is a cube with a side length of 0.6 m.

3.2 *Distortion correction*

The self-pose of the motorcycle is calculated every 100 ms (LiDAR scan period) based on NDT map

matching. The scan data is acquired 180 times every 0.55 ms during LiDAR scanning. During LiDAR scanning, all the scan data within one scan cannot be obtained at the same time when the motorcycle is moving or changing its attitude. Therefore, if entire scan data within one scan are mapped onto the world coordinate frame based on the pose of the motorcycle at a single time, distortion arises in the mapping.

Therefore, the distortion in the scan data is corrected by EKF [15]. Fig. 3 shows the flow of distortion correction of LiDAR scan data. The LiDAR scan period (100 ms) is denoted as τ, the IMU observation period (10 ms) as $\Delta\tau_{IMU}$, and the scan data observation period (0.55 ms) as $\Delta\tau$. The method of correcting distortion in the scan data obtained from time $(t-1)\tau+\Delta\tau$ to $(t-1)\tau+180\Delta\tau$ $(=t\tau)$ is hereby described.

Using the information from the pose of the motorcycle obtained by NDT map matching every τ and the IMU information obtained every $\Delta\tau_{IMU}$, the EKF estimates the poses $\hat{\boldsymbol{X}}^{(k-1)}(t-1)$ at the time $(t-1)\tau+(k-1)\Delta\tau_{IMU}$ and $\hat{\boldsymbol{X}}^{(k)}(t-1)$ at $(t-1)\tau+k\Delta\tau_{IMU}$ $(=(t-1)\tau+(k-1)\Delta\tau_{IMU}+18\Delta\tau)$, where $k=1$–10.

From these estimates, the self-pose $\hat{\boldsymbol{X}}^{(k-1)}(t-1,j)$ at $(t-1)\tau+(k-1)\Delta\tau_{IMU}+j\Delta\tau$ (where j = 1–17) is interpolated. The scan data $\boldsymbol{p}_{bi}^{(k-1)}(t-1,j)$ (where i = 1, 2, …, n) obtained at $(t-1)\tau+(k-1)\Delta\tau_{IMU}+j\Delta\tau$ is transformed to $\boldsymbol{p}_{i}^{(k-1)}(t-1,j)$ as follows:

$$\begin{pmatrix}\boldsymbol{p}_{i}^{(k-1)}(t-1,j)\\1\end{pmatrix}=T(\hat{\boldsymbol{X}}^{(k-1)}(t-1,j))\begin{pmatrix}\boldsymbol{p}_{bi}^{(k-1)}(t-1,j)\\1\end{pmatrix} \quad (3)$$

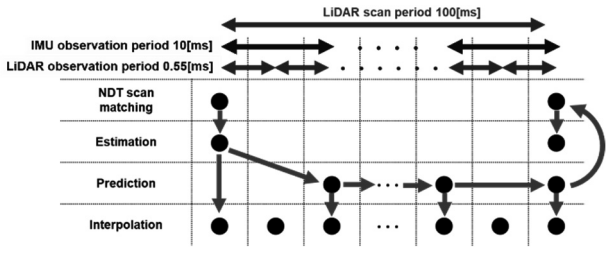

Fig. 3. Flow of distortion correction.

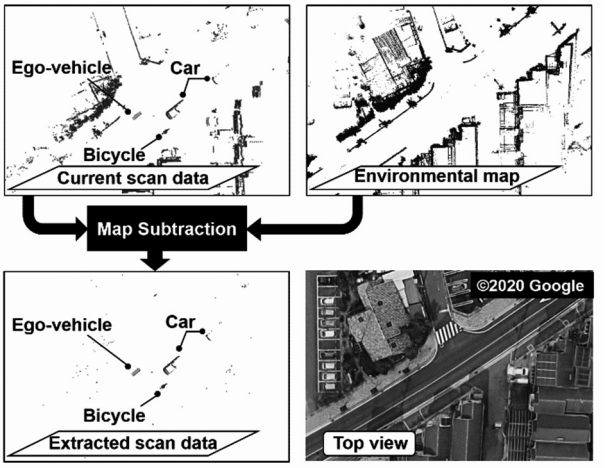

Fig. 4. Map-subtraction method.

Using the pose estimate $\hat{\boldsymbol{X}}^{(10)}(t-1)$ at $t\tau$ $(=(t-1)\tau+10\Delta\tau_{IMU})$, the scan data $\boldsymbol{p}_{i}^{(k-1)}(t-1,j)$ in the world coordinate frame is again transformed to the scan data $\boldsymbol{p}_{bi}^{*}(t)$ in the sensor coordinate frame at $t\tau$ by

$$\begin{pmatrix}\boldsymbol{p}_{bi}^{*}(t)\\1\end{pmatrix}=T(\hat{\boldsymbol{X}}^{(10)}(t-1))^{-1}\begin{pmatrix}\boldsymbol{p}_{i}^{(k-1)}(t-1,j)\\1\end{pmatrix} \quad (4)$$

$\boldsymbol{p}_{bi}^{*}(t)$ obtained by Eq. (4) is the scan data, in which distortion is corrected. For the EKF, a constant velocity model is used as the motion of the motorcycle [15].

4. Moving-Object Detection and Tracking

Fig. 4 shows the flow of map-subtraction method. The scan data corrected by Eq. (4) at the current scan (current scan data) are matched with the environment map using NDT map matching, and the scan data is subtracted by comparing the current scan data with the environmental map.

An elevation map is applied to detect moving objects; the scan data extracted based on map-subtraction are mapped onto the elevation map represented in the world coordinate frame. In this study, the cell of the elevation map is a square with a side length of 0.3 m.

A cell in which scan data exist is called an occupied cell. For scan data related to moving objects (moving scan data), the time to occupy the same cell is short, whereas for scan data related to static objects (static scan data), the

time is long. Therefore, by using the occupancy grid method based on the cell occupancy time [4], cells that are occupied by the moving scan data are detected (moving cells) and clustered (moving-cell group).

When moving-object detection is completed, tracking (estimating position, velocity, and size) of moving objects is performed[5]. In this paper, the shape of a tracked object is represented by a cuboid with a width W, a length L, and a height H as shown in Fig. 5.

As shown in Fig. 6, an X_vY_v-coordinate frame, on which the Y_v-axis aligns with the heading of a tracked object is defined. From clustered moving cells, the width W_{meas} and length L_{meas} are measured.

When a moving object is perfectly visible, its size can accurately be estimated from the measurements W_{meas} and L_{meas}. In contrast, when it is partially occluded by other objects, its size is incorrectly estimated. Therefore, the size of a partially visible object is estimated using the following equation:

$$\begin{cases} W(t) = W(t-1) + G(W_{meas} - W(t-1)) \\ L(t) = L(t-1) + G(L_{meas} - L(t-1)) \end{cases} \quad (5)$$

where t and t-1 are time steps. G is the filter gain. The height of the moving-cell group uses as the height estimate H.

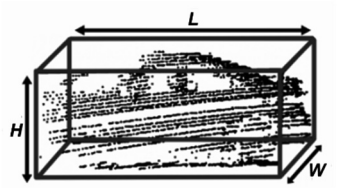

Fig. 5. Cuboid around the tracked object (car).

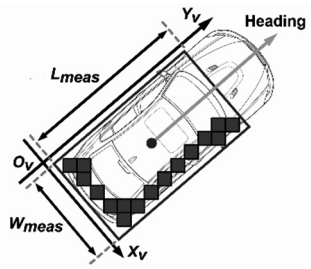

Fig. 6. Estimated size. Squares and arrow indicate moving cells and vehicle heading direction, respectively. Rectangle and circle indicate estimated size and centroid.

The centroid position of the rectangle estimated from Eq. (5) is define by (x, y) in the world coordinate frame. From the centroid position, the position and velocity of the object are estimated in the world coordinate frame using the Kalman filter under the assumption that the object is moving at an almost constant velocity [5].

To track objects in crowded environments, data association (i.e., one-to-one or one-to-many matching of tracked objects and moving-cell groups) is needed. The global-nearest-neighbor (GNN) based and rule-based data association are utilized to accurately perform data association [5].

5. Experimental Results

Two experiments are conducted using sensor data sets in ref. 18) to validate the effectiveness of the proposed method. The first experiment (experiment 1) is conducted on a public road, as shown in Fig. 7 (a). The maximum speed of the motorcycle is 40 km/h, and the distance traveled is 1200 m. On the road, there are 18 pedestrians, 15 two-wheeled vehicles, and 38 cars.

Fig. 8 shows the tracking results of moving objects in the intersection shown in Fig. 7 (b). The rectangle indicates the estimated size of the moving object, and the stick at the rectangle indicates the moving direction of the moving object obtained from the velocity estimate. The black dots indicate the LiDAR scan data Fig. 9 shows the attitude angles and angular velocities of the motorcycle moving in the intersection.

When the motorcycle turns left at the intersection, the maximum roll angle is 10°, and the maximum roll angular velocity is 14.5°/s. It is clear from Fig. 8 that even when the motorcycle attitude changes significantly by turning left, static data originating from building walls and stopped car are removed, and the moving objects are tracked.

The motorcycle was moved three times on the road shown in Fig. 7 (a). Total number of moving objects are

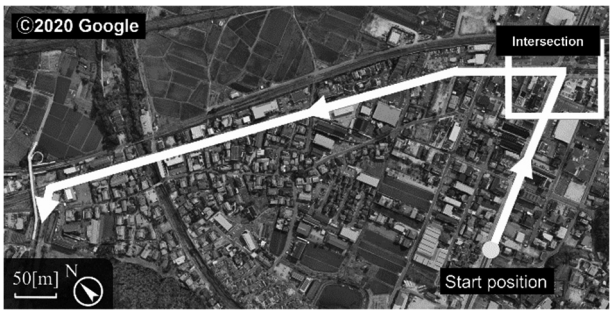

(a) Overall

(b) Intersection

Fig. 7. Photo (top view) of the environment (experiment 1). The white line indicates the movement path of the ego-vehicle (motorcycle).

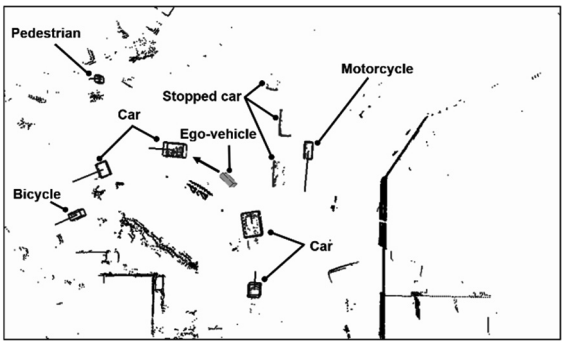

Fig. 8. Estimated track and size of the moving objects (top view).

211 (133 cars, 28 two-wheeled vehicles, and 50 pedestrians). We compare the tracking performance in the following cases.

Case 1: Tracking with distortion correction and map subtraction (proposed method),

Case 2: Tracking with distortion correction and without map subtraction,

Case 3: Tracking with map subtraction and without distortion correction, and

Case 4: Tracking without either method.

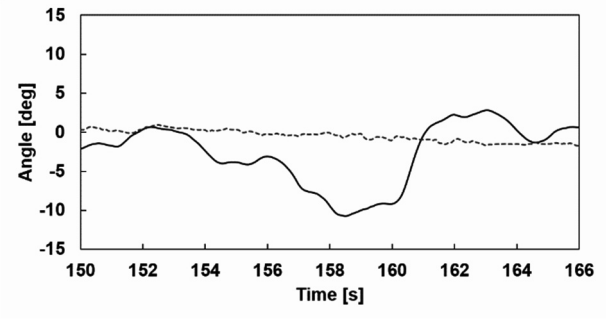

(a) Roll (bold line) and pitch (dashed line) angles

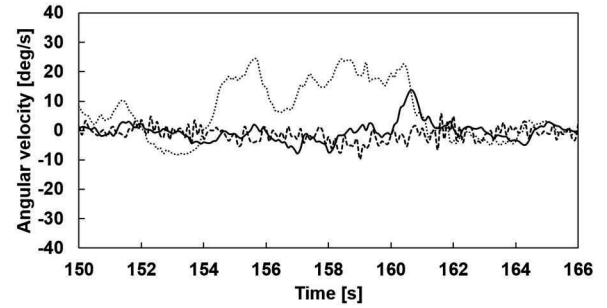

(b) Roll (bold line), pitch (dashed line), and yaw (dotted line) angular velocities

Fig. 9. Attitude angle and angular velocity of the ego-vehicle (experiment 1).

Table 1. Total number of correct and incorrect tracking (experiment 1).

	Correct tracking	Untracking	False tracking
Case 1	210	1	18
Case 2	210	1	34
Case 3	208	3	153
Case 4	209	2	40

Table 1 shows the tracking result, where untracking means that tracking of moving objects fails, and false tracking means that static objects are tracked. It is clear from the table that the proposed method (case 1) provides the tracking performance better than the other cases.

Since experiment 1 is conducted on a public road, the motorcycle attitude is significantly changed only when turning at intersection shown in Fig. 7 (b). Therefore, to investigate tracking performance when the motorcycle experiences a large attitude change, another

Fig. 10. Photo (bird's-eye view) of the environment (experiment 2). The white line indicates the movement path of the ego-vehicle (motorcycle).

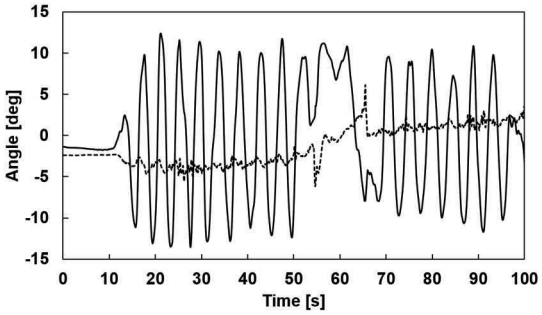

(a) Roll (bold line) and pitch (dashed line) angles

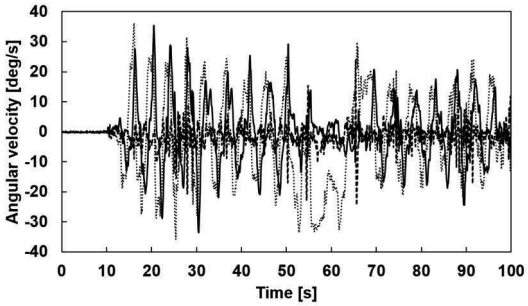

(b) Roll (bold line), pitch (dashed line), and yaw (dotted line) angular velocities

Fig. 11. Attitude angle and angular velocity of the ego-vehicle (experiment 2).

Table 2. Total number of correct and incorrect tracking (experiment 2).

	Correct tracking	Untracking	False tracking
Case 1	236	1	3
Case 2	235	2	8
Case 3	232	5	51
Case 4	232	5	25

experiment (experiment 2) is conducted on our university campus, where the motorcycle is frequently ridden in zigzag paths. Fig. 10 shows the movement path of the motorcycle. The distance traveled by the motorcycle is 500 m, and the maximum speed is 25 km/h. The attitude angle and angular velocity of the motorcycle are shown in Fig. 11. The motorcycle was moved five times on the road. Total number of moving objects are 237 (10 cars and 227 pedestrians).

Table 2 shows the tracking result. From this table, it can be seen that our proposed method (case 1) can reduce the amount of false tracking even when large swing motion of motorcycle.

6. Conclusions and Future Works

This paper presented a moving-object tracking method with the motorcycle-mounted scanning LiDAR in GNSS-denied environments. The distortion in scan data from the scanning LiDAR was corrected by estimating the pose of the motorcycle in a period shorter than the LiDAR scan period using NDT based map matching and the IMU information via EKF.

By comparing the corrected LiDAR scan data with the environment map via the NDT scan matching, the scan data of interest were extracted and mapped onto the elevation map to detect and track moving objects. Experimental results obtained in public road and university-campus road environments by a 32-layer LiDAR mounted on a motorcycle showed that the distortion correction in LiDAR scan data and map subtraction could provide the tracking accuracy better than conventional methods.

Although the map-subtraction method can improve the tracking performance, it requires an environment map in advance. To enable the accurate tracking of moving objects in first-visit environments, we presented a dynamic background subtraction (DBS)-based extraction method[18], where a local map was sequentially built using NDT-based SLAM, and the scan data of interest were

extracted by subtracting the local map from the current LiDAR scan data. As a further work on moving-object tracking, we need to compare the tracking performance of the map-subtraction based method proposed in this paper and the DBS-based extraction method through detailed experiments under various traffic environments.

Our contribution of this paper is also the accurate tracking of moving objects even in large swing motion of the LiDAR. As future works, we will thus extend the proposed method to moving-object tracking using LiDAR mounted on vehicles and robots that swing motion frequently occurs, such as narrow tilting vehicles, uneven terrain vehicles, walking robots, and drones.

This study was partially supported by the KAKENHI Grant #18K04062, the Japan Society for the Promotion of Science (JSPS).

References

1) A. Mukhtar, L. Xia, and T. B. Tang, "Vehicle Detection Techniques for Collision Avoidance Systems: A Review," *IEEE Trans. Intelligent Transportation Systems*, **16**, 2318–2338 (2015).

2) E. Marti, J. Perez, M. A. Miguel, and F. Garcia, "A Review of Sensor Technologies for Perception in Automated Driving," *IEEE Intelligent Transportation Systems Magazine*, 94–108 (2019).

3) F. P. Muller, "Survey on Ranging Sensors and Cooperative Techniques for Relative Positioning of Vehicles," *Sensors*, **17** (2017).

4) M. Hashimoto, S. Ogata, F. Oba, and T. Murayama, "A Laser Based Multi-Target Tracking for Mobile Robot," *Intelligent Autonomous Systems* **9**, 135–144 (2006).

5) Y. Tamura, R. Murabayashi, M. Hashimoto, and K. Takahashi, "Hierarchical Cooperative Tracking of Vehicles and People Using Laser Scanners Mounted on Multiple Mobile Robots," *Int. J. Advances in Intelligent Systems*, **10**, 90–101 (2017).

6) A. Amodio, G. Panzani, and S. M. Savaresi, "Design of a Lane Change Driver Assistance System with Implementation and Testing on Motorbike," *Proc. IEEE Intelligent Vehicles Symp.*, 947–952 (2017).

7) Z. Xie and R. Rajamani, "On-Bicycle Vehicle Tracking at Traffic Intersections Using Inexpensive Low-Density Lidar," *Proc. American Control Conf.*, 953–958 (2019).

8) G. Gil, G. Savino, S. Piantini, and M. Pierini, "Motorcycles that See: Multifocal Stereo Vision Sensor for Advanced Safety Systems in Tilting Vehicles," *Sensors*, **18** (2018).

9) W. Jeon and R. Rajamani, "Rear Vehicle Tracking on a Bicycle Using Active Sensor Orientation Control," *IEEE Trans. Intelligent Transportation Systems*, **19**, 2638–2649 (2018).

10) S. Thrun, W. Burgard, and D. Fox, "Probabilistic Robotics," *MIT press* (2005).

11) K. Inui, M. Morikawa, M. Hashimoto, K. Tokorodani, and K. Takahashi, "Distortion Correction of Laser Scan Data from In-Vehicle Laser Scanner Based on NDT Scan-Matching," *Proc. 14th Int. Conf. Informatics in Control, Automation and Robotics*, 329–334 (2017).

12) S. Muro, Y. Matsui, M. Hashimoto, and K. Takahashi, "Moving-Object Tracking with Lidar Mounted on Two-Wheeled Vehicle," *Proc. 16th Int. Conf. on Informatics in Control, Automation and Robotics*, 453–459 (2019).

13) K. Matsuo, A. Yoshida, M. Hashimoto, and K. Takahashi, "NDT Based Mapping Using Scanning Lidar Mounted on Motorcycle," *Proc. Fifth Int. Conf. Advances in Sensors, Actuators, Metering and Sensing*, 69–75 (2020).

14) S. Tanaka, C. Koshiro, M. Yamaji, M. Hashimoto, and K. Takahashi, "Point Cloud Mapping and Merging in GNSS-Denied and Dynamic Environments Using Only Onboard Scanning LiDAR," *Int. J. Advances in Systems and Measurements*, **13**, 275–288 (2020).

15) K. Tokorodani, M. Hashimoto, Y. Aihara, and K. Takahashi, "Point-Cloud Mapping Using Lidar Mounted on Two-Wheeled Vehicle Based on NDT Scan Matching," *Proc. 18th Int. Conf. Informatics in Control, Automation and Robotics*, 446–452 (2019).

16) P. Biber and W. Strasser, "The Normal Distributions Transform: A New Approach to Laser Scan Matching," *Proc. IEEE/RSJ Int. Conf. Intelligent Robots and Systems*, 2743–2748 (2003).

17) M. Munaro, F. Basso, and E. Menegatti, "Tracking People within Groups with RGB-D Data," *Proc. IEEE/RSJ Int. Conf. on Intelligent Robots and Systems*, 2101–2107 (2012).

18) S. Muro, I. Yoshida, M. Hashimoto, and K. Takahashi, "Moving-Object Tracking by Scanning LiDAR Mounted on Motorcycle Based on Dynamic Background Subtraction," *Artificial Life and Robotics*, **26**, 412–422 (2021).